Dependence of Turing pattern wavelength on diffusion rate

Qi Ouyang
Center for Nonlinear Dynamics and Department of Physics, The University of Texas at Austin, Austin, Texas 78712

Rusheng Li and Ge Li
Department of Chemistry, The Tsinghua University, Beijing 10008, The People's Republic of China

Harry L. Swinney
Center for Nonlinear Dynamics and Department of Physics, The University of Texas at Austin, Austin, Texas 78712

(Received 12 September 1994; accepted 31 October 1994)

The relation between the diffusion coefficient of reactants and the wavelength of Turing patterns is examined in experiments on the chlorite–iodide–malonic acid (CIMA) reaction in gel media. The diffusion coefficients in polyacrylamide and agarose gels are varied by varying the gel densities. The diffusion coefficient D of NaCl is found to vary from 0.5×10^{-5} to 1.8×10^{-5} cm^2/s for the gel conditions considered. The CIMA reactants are assumed to have diffusion coefficients that are directly proportional to that of NaCl. The wavelength λ of the observed hexagonal patterns (0.13–0.28 mm) varies in accord with the predicted relation for Turing patterns, $\lambda\sim D^{1/2}$. Moreover, the predicted relationship to a characteristic period of oscillation τ, $\lambda=(2\pi\tau D)^{1/2}$, is supported by measurements of τ just beyond a Hopf bifurcation in a stirred flow reactor. © *1995 American Institute of Physics.*

I. INTRODUCTION

A defining of property of Turing patterns (reaction-diffusion spatial patterns arising from an instability in a uniform medium) is the square root dependence of the wavelength of the pattern on the diffusion coefficient of the reactants.[1] This relationship was predicted by Turing in his classic paper more than 40 years ago[1] and has been discussed by many authors[2–5] but never tested in experiments. Near the bifurcation from a uniform state to patterns the pattern wavelength λ is predicted to be[6]

$$\lambda=(2\pi\tau D)^{1/2}, \tag{1}$$

where τ is the period of the limit cycle oscillation when the system is at the onset of Hopf bifurcation, and D is the average diffusion coefficient of reactants (see the Appendix).

The first observation of a stationary Turing structure in sustained nonequilibrium conditions was reported in 1990 by a group led by De Kepper using a chlorite–iodide–malonic acid (CIMA) reaction.[7] Subsequently a clear demonstration of a Turing bifurcation was obtained by two of us using the same reaction system.[8] However, direct evidence of the square-root dependence of Turing pattern wavelength on the diffusion coefficient has been lacking, although indirect evidence has been reported.[7,9] The present experiments were undertaken to test (1) in direct measurements of λ, D, and τ.

The essential idea of our experiments is to vary the diffusion rate of reactants by using different gels as the reaction media. We use two types of gels, polyacrylamide and agarose. The pores in a polyacrylamide gel are typically 80 Å in diameter, while the pores in an agarose gel are typically 5000 Å;[9] hence the diffusion rates are smaller in a polyacrylamide gel than in an agarose gel. In addition to using two types of gel, we vary the diffusion rate in each gel by varying the concentration of acrylamide or agarose used to prepare the gels. The diffusion coefficients are found to vary by a factor of 3 for the conditions considered. The period of oscillation in a stirred flow reactor is found to be in the range 9–60 s, depending on malonic acid concentration. The independent measurements of λ, D, and τ are in reasonable accord with Eq. (1).

II. EXPERIMENTAL METHODS

A. Reaction-diffusion system

The measurements of the diffusion coefficient of a chemical in the reaction medium and of the wavelength of Turing patterns are conducted in the same spatial open reactor, shown in Fig. 1. The core of the reactor is a thin gel disk, 25.4 mm in diameter and 1.0–1.6 mm thick, made of polyacrylamide or agarose. The polyacrylamide gel was prepared by the procedure described in Ref. 7. The agarose gel was prepared by dissolving 0.1–2.0 g agarose (Sigma) in 20 mL 80 °C water, and then casting the solution between two glass plates with spacers at room temperature. The gels prevent convective motion in the reaction medium. Both the polyacrylamide and agarose gels are assumed to be inert to the reactants for our experimental conditions—inspection of the gels after continuous experiments for six weeks revealed no visible chemical or physical changes. To visualize Turing patterns formed in the gels, some soluble starch, an indicator for the CIMA reaction,[10] is loaded into a gel during preparation.

A gel is held rigidly either between two Anopore aluminum oxide disks (0.06 mm thick, 25.4 mm diam, from Whatman) or between two porous glass disks (0.4 mm thick, 25.4 mm diam, Vycor glass from Corning). The outer flat surface of each membrane disk is in contact with a continuous flow stirred tank reactor (CSTR) of 7.3 mL volume that is fed

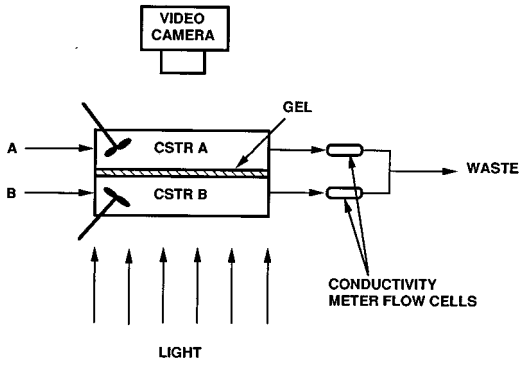

FIG. 1. Schematic diagram of the open spatial reactor. Patterns form in the gel that is sandwiched between the continuous flow stirred reservoirs (CSTRs) *A* and *B*.

with chemicals by Pharmacia P-500 precision pumps. The reactor temperature for the studies of patterns is 7 °C.

Our pattern forming experiments use a chlorite–iodide–malonic acid (CIMA) reaction in an acidic (sulfuric acid) aqueous solution.[11] Components of the reaction are fed into CSTRs *A* and *B* in such a way that there are opposing gradients of chlorite and malonic acid; chlorite is only in CSTR *A*, and malonic acid is only in CSTR *B* (see Fig. 1). The other chemical species are fed in equal amounts in both CSTRs, except for sulfuric acid, which is more concentrated in *B* than in *A*. The Vycor porous glass disks are used in measurements of the wavelength of Turing patterns. We measured the diffusion rate of NaCl in Vycor glass to be 7×10^{-7} cm^2/s, which is 8–20 times slower than that in the gels. Thus most of the chemical gradients are in the Vycor glass disks rather than in the gel; this minimizes the influence of the gradients on the wavelength of Turing patterns. The chemicals diffuse from the CSTRs, through Vycor glass disks, and into the gel medium where the CIMA reaction occurs and Turing patterns form. For each set of experiments, the chemical patterns are allowed to develop for at least 12 h before the images of patterns are recorded. For our experimental conditions, the wavelength selection process is completed within 4 h from the beginning of an experiment; the local domain structures, which extend typically ten wavelengths, become stationary after about 12 h. A Sanyo video camera fitted with a macro lens is used to detect the intensity of transmitted light as a function of position in the plane of the gel. The video output is digitized by a personal computer equipped with a frame grabber. The wavelength of the patterns is determined from fast Fourier transforms.

B. Diffusion coefficient measurements

We chose NaCl as a neutral chemical and measured the diffusion coefficient in different media. For these measurements the outlet of each CSTR was connected to a flow cell with a conductivity meter (Model 1481-60, Cole Parmer), and the two outflows were connected together before emptying into the waste tank (see Fig. 1). The connection of the waste lines eliminated any pressure difference between the two CSTRs due to fluctuations of the pumps, thus preventing nondiffusive mass flow across the gel. Saline solution (0.01 M) was fed into CSTR *A* with a flow *f* rate of 40 mL/h, and water was fed into CSTR *B* with the same flow rate. Thus the mass balance equations in CSTRs *A* and *B* are, respectively,

$$dC_A/dt = f(C_0 - C_A) - JS, \tag{2}$$

$$dC_B/dt = JS - fC_B, \tag{3}$$

where C_A, C_B, and C_0 are, respectively, the concentrations of NaCl in CSTR *A*, in CSTR *B*, and of the inlet solution in CSTR *A*; *S* is the area of the gel disk in contact with the CSTRs; and *J* is the flux through the gel/Anopore membrane sandwich.

At equilibrium we have

$$J = D_s(C_A - C_B)/h, \tag{4}$$

where D_s is the average diffusion coefficient of NaCl in the gel/Anopore sandwich, and *h* is the thickness of the gel/Anopore sandwich. Substituting Eq. (4) into Eqs. (2) and (3), we obtain D_s in terms of measured quantities,

$$D_s = fhC_B/(C_A - C_B)S. \tag{5}$$

Because the Anopore membrane has a large pore size (20 μm), the diffusion coefficient of NaCl in the membrane can be assumed to be the same as in water, 1.8×10^{-5} cm^2/s.[12] Thus the diffusion coefficient of NaCl in the gel media can be obtained from following relations:

$$h/D_s = h_m/D_m + h_g/D_g, \tag{6}$$

$$h = h_m + h_g, \tag{7}$$

where D_m and D_g are, respectively, the diffusion coefficients of NaCl in Anopore and gel media, and h_m and h_g are the thicknesses of the Anopore and gel membranes.

The values of C_A and C_B were obtained from the readings of conductivity meters in *A* and *B*. Each conductivity meter was calibrated with standard NaCl solutions; the relative error was about 0.5%. The flow rate was controlled within 0.2% by the precision pumps. The value of *S* was 3.24 ± 0.01 cm^2, and *h*, measured to ±0.02 mm, was in the range 1.0–1.8 mm. Thus our diffusion coefficient values for NaCl in a gel medium have an error less than 5%.

Since the polyacrylamide and agarose gels are assumed to be inert both to the reactants of the CIMA reaction and to the NaCl, it is reasonable to assume that the diffusion coefficients of the CIMA reactants behave in the same way as that of NaCl in the gels. Hence in all the reaction media we assume that the ratio of the average diffusion coefficient of the CIMA reactants to the diffusion coefficient of NaCl is constant. In the calculation of Hopf period of the CIMA reaction, we take the constant ratio to be unity [see Eq. (8) in Sec. III].

Figure 2 shows an example of the time evolution of NaCl concentration. The system nearly reaches a steady state in 2–3 h, but to be assured of asymptotic behavior, we made measurements for eight or more hours after each change in concentration.

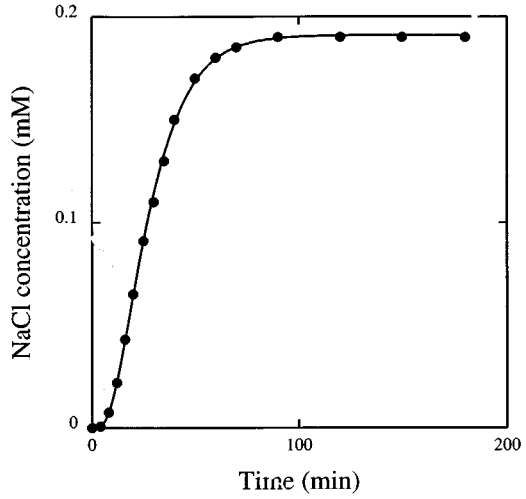

FIG. 2. Time evolution of NaCl concentration in CSTR *B* after the start of an experiment using an agarose gel (1.8 mm thick) and a NaCl concentration of 10 mM in CSTR *A*. The residence time of each CSTR is 11 min.

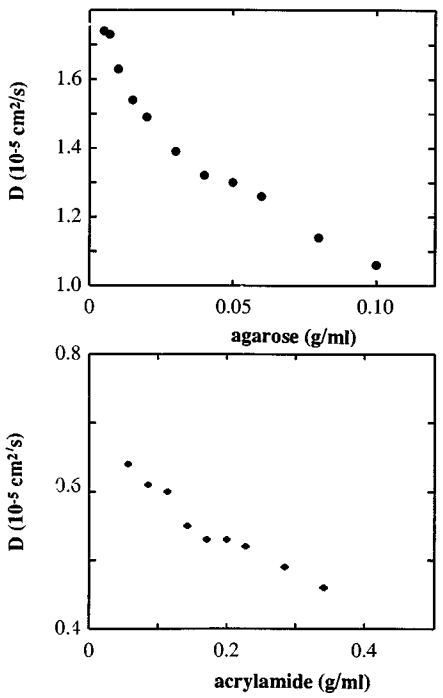

FIG. 4. Diffusion coefficient of NaCl as a function of the gel density in (a) an agarose gel and (b) a polyacrylamide gel. The temperature is 25 °C.

III. RESULTS

Figure 3 shows examples of Turing patterns observed for the same chemical conditions but with different gel media. Figure 3(a) was obtained for a polyacrylamide gel, and Figs. 3(b) and 3(c) were obtained for agarose gels with different densities. All three patterns consist of domains of hexagonal structures, but the wavelengths are quite different. Shortly after the beginning of the experiment, hundreds of light circles appear and grow in a dark background. Within an hour these small target patterns break into light dots that evolve slowly. Initially there is a broad distribution of sizes of the light dots, but the dots become more and more uniform in size as the linear wavelength selection process proceeds.[13] After 3–4 h, the dots have evolved to local hexagonal structures. There is no further evolution in the pattern wavelength, as determined from spatial Fourier spectra—wavelengths determined at 5 and 24 h are the same within the experimental uncertainty, 2%. However, the pattern continues to evolve on a slow time scale into hexagonal, striped, or rhombic lattices, depending on boundary and initial conditions, as the nonlinear selection process begins to dominate the pattern evolution.[13,14]

The results of the diffusion coefficient measurements in different gel media are summarized in Fig. 4. The diffusion rate of NaCl decreases monotonically with increasing density

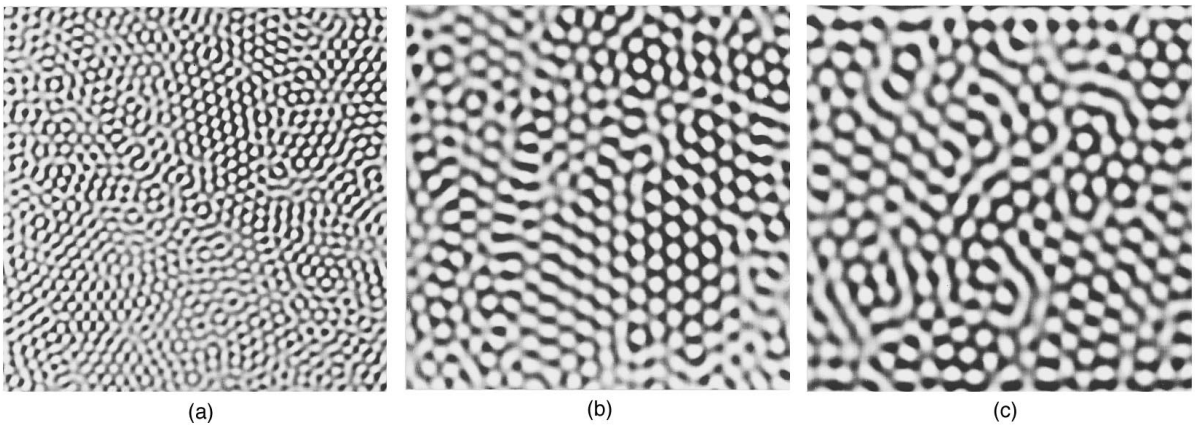

FIG. 3. Stationary hexagonal patterns formed in (a) a polyacrylamide gel; (b) a high density agarose gel; and (c) a low density agarose gel. A 5.0×5.0 mm^2 region is shown in each figure. The diffusion coefficients in the gels are, respectively, 0.5×10^{-5} cm^2/s, 1.1×10^{-5} cm^2/s, and 1.80×10^{-5} cm^2/s; the corresponding pattern wavelengths are 0.13 mm, 0.22 mm, and 0.28 mm. The reagent conditions are held fixed: $[I^-]_0^A=[I^-]_0^B=3$ mM, $[Na_2SO_4]_0^A=3$ mM, $[ClO_2^-]_0^A=17$ mM, $[NaOH]_0^A=2$ mM, $[H_2SO_4]_0^A=2$ mM, $[CH_2(COOH)_2]_0^B=13$ mM, $[H_2SO_4]_0^B=20$ mM. The residence time of each CSTR is 11 min, and the temperature is held fixed at 7 °C.

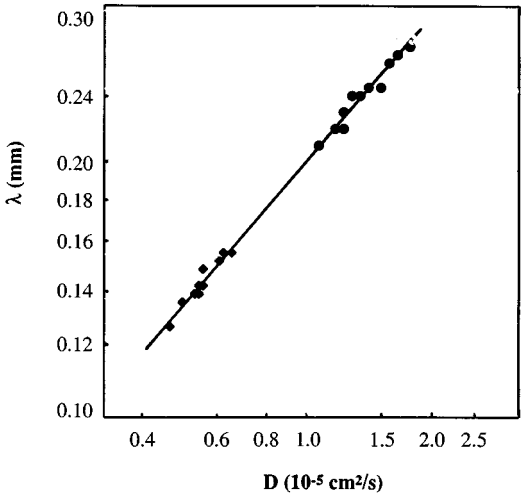

FIG. 5. A log–log plot of the wavelength of the Turing patterns as a function of the average diffusion coefficient of reactants in that medium; ◆, polyacrylamide gel; ●, agarose gel. The solid line, a least-squares fit to the data, has slope 0.54±0.10. The reaction conditions are the same as in Fig. 3.

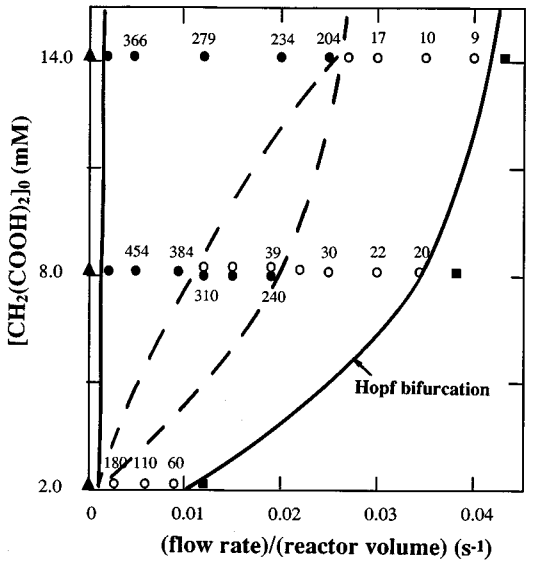

FIG. 6. States of the chlorite–iodide–malonic acid reaction in a CSTR as function of malonic acid feed concentration and flow rate, with other feed concentrations held fixed; $[I^-]_0$=3.5 mM, $[ClO_2^-]_0$=6 mM, $[H_2SO_4]_0$=5 mM, $[NaOH]_0$=2 mM, T=25 °C. Symbols, ■, oxidized state; ▲, reduced state; ○, sinusoidal oscillations; ●, relaxational oscillations. The numbers in the figure are the oscillation periods in seconds.

of the agarose gel, decreasing from 1.8×10^{-5} to 1.09×10^{-5} cm^2/s for gel concentration increasing from 0.5% to 10% (w/w). The diffusion rate measured in the least dense agarose gel (0.5% concentration) is the same as for NaCl in pure water.[12] Agarose concentrations higher than 10% could not be used because the gel solution became so viscous that it trapped air bubbles, making the gel inhomogeneous.

As expected, NaCl diffuses more slowly in polyacrylamide gel than agarose gel. In a polyacrylamide gel the diffusion coefficient of NaCl decreases from 0.64×10^{-5} to 0.46×10^{-5} cm^2/s when the acrylamide density is increased from 5.7% (w/w) to 34.2% (w/w). The lower end in acrylamide density is limited by the concentration required for acrylamide to polymerize; the higher end in density is limited by the solubility of acrylamide.

Figure 5 is a plot of the wavelength of the Turing patterns as a function of diffusion coefficient. With the assumption that the CIMA reactants behave the same as NaCl in the gel media, the straight line fit to the data on the log–log plot yields

$$\lambda = \beta D^{\alpha}, \tag{8}$$

where λ is the wavelength of the Turing pattern, D is the average diffusion coefficient of the reactants, and α and β are constants. The value of α in our experiments is 0.54 ±0.10 (including systematic as well as statistical uncertainties), in accord with the predicted value of 1/2 (see the Appendix). These measurements provide the first direct evidence for the square root dependence of wavelength of Turing patterns on the diffusion coefficient of reactants.

The value of β determined from the least-squares fit, assuming α=1/2, is 6.7±0.5 (with λ in cm and D in cm^2/s). From Eq. (1) we have

$$\beta = (2\pi\tau/f)^{1/2}, \tag{9}$$

where f is the ratio of diffusion coefficient values at 25 and at 7 °C (the factor f arises because the diffusion coefficient and Turing pattern measurements were made at different temperatures, 25 and 7 °C, respectively). The value of f estimated from the approximate calculation of Lengyel and Epstein[15] is 2. We thus deduce that the period τ of the limit-cycle oscillation at the onset of Hopf bifurcation should be ~14 s. Our wavelength measurements were made in a Turing regime near a Turing–Hopf bifurcation.[9] We also have measured the period of oscillations near a Hopf bifurcation of the CIMA reaction in a CSTR and have found that the oscillation period at onset of Hopf bifurcation is between 9 and 60 s, depending on malonic acid concentration (see Fig. 6). The direct measurement of the oscillation period at the onset is consistent with an estimate of 16 s deduced from Eq. (1).

IV. CONCLUSION

The square-root dependence of the wavelength of Turing patterns on the diffusion coefficient of the reactants has long been predicted[1–6] and has been a defining property for Turing structures. Our evidence of the square-root dependence of the Turing wavelength on the diffusion rate indicates that the patterns observed in the CIMA reaction are indeed Turing patterns.

ACKNOWLEDGMENTS

We thank M. Florian, K. J. Lee, and W. D. McCormick for helpful discussions. This work was supported by the Department of Energy Office of Basic Energy Sciences. Q.O. is partly supported by the China-Cornell Fellowship program.

APPENDIX: TURING INSTABILITY AND TURING PATTERN WAVELENGTH

A reaction-diffusion system can be described by

$$\partial C_i/\partial t = D_i \nabla^2 C_i + f_i(\ldots, C_i, \ldots, C_j, \ldots), \tag{A1}$$

where C_i is the chemical concentration of the ith species participating in the reaction described by the nonlinear function, f_i, and D_i is the diffusion coefficient of species i. Assuming that Eq. (A1) has a homogenous steady state solution, $f_i(C_s)=0$, we consider the evolution of a small perturbation c_s around C_s and separate it in Fourier space,

$$c_s = \sum_k a_k e^{\lambda_k t + i\mathbf{k}\cdot\mathbf{r}}, \tag{A2}$$

where λ_k is the growth rate of the mode with a wave vector $\mathbf{k}$. Substituting Eq. (A2) into Eq. (A1) and retaining only the linear term, we obtain an eigenvalue equation for λ_k for the linear operator

$$L_{ij} = F_{ij} - D_i k^2 \delta_{ij}, \tag{A3}$$

where F_{ij} is the Jacobian matrix $(\partial f_i/\partial c_j)_{c=c_s}$ of the kinetic function f_i. Turing instability occurs when for a certain nonzero mode k, the real part of the eigenvalue λ_k of the operator (A3) becomes positive so that the homogeneous steady state becomes unstable, and the system undergoes a transition from the homogeneous state to a patterned state.

Consider a two-variable system. A Hopf bifurcation of the homogenous system occurs when

$$\mathrm{Tr}\ \mathbf{F} = F_{11} + F_{22} = 0 \tag{A4}$$

with the frequency of the oscillation

$$\omega_H = (|\mathbf{F}|)^{1/2} \neq 0, \tag{A5}$$

where $|\mathbf{F}| = F_{11}F_{22} - F_{12}F_{21}$. A Turing bifurcation occurs when a certain nonzero mode k of the perturbation (A2) goes unstable as a parameter is varied while the $k=0$ mode remains stable. This occurs when

$$\Delta(k^2) = |\mathbf{F}| - (D_1 F_{22} + D_2 F_{11})k^2 + D_1 D_2 k^4 = 0, \tag{A6}$$

provided that

$$D_2 F_{11} + D_1 F_{22} > 0, \quad F_{11} + F_{22} < 0. \tag{A7}$$

The critical wavelength is determined by the degenerate root of Eq. (A6). Thus we have

$$(D_1 F_{22} + D_2 F_{11})^2 = 4 D_1 D_2 |\mathbf{F}|. \tag{A8}$$

Combining Eqs. (A6) and (A8), we get the critical wave number at the onset of a Turing pattern,

$$k_c^2 = [|\mathbf{F}|/(D_1 D_2)]^{1/2}. \tag{A9}$$

Since the critical Turing pattern wavelength is $\lambda_c = 2\pi/k_c$, the average diffusion coefficient is $D = (D_1 D_2)^{1/2}$, and the Hopf period is $\tau = 2\pi/\omega_H = 2\pi/(|\mathbf{F}|)^{1/2}$, the relation between the Turing pattern wavelength and the diffusion coefficient of the system is

$$\lambda_c = (2\pi\tau D)^{1/2}. \tag{A10}$$

[1] A. M. Turing, Philos. Trans. R. Soc. London, Ser. B **327**, 37 (1952).
[2] G. Nicolis and I. Prigogine, *Self-organization in Nonequilibrium Chemical Systems* (Wiley, New York, 1977).
[3] H. Meinhardt, *Models of Biological Pattern Formation* (Academic, New York, 1986).
[4] J. D. Murray, *Mathematical Biology* (Springer, New York, 1989).
[5] L. G. Harrison, *Kinetic Theory of Living Pattern* (Cambridge University, Cambridge, 1992).
[6] J. E. Pearson, Physica A **188**, 178 (1992); J. E. Pearson and W. J. Bruno, Chaos **2**, 513 (1992).
[7] V. Castets, E. Dulos, J. Boissonade, and P. De Kepper, Phys. Rev. Lett. **64**, 2953 (1990).
[8] Q. Ouyang and H. L. Swinney, Nature **352**, 610 (1991); in *Chemical Waves and Patterns*, edited by R. Kapral and K. Showalter (Kluwer, Dortrecht, 1994).
[9] J. Boissonade, E. Dulos, and P. De Kepper, in *Chemical Waves and Patterns*, edited by R. Kapral and K. Showalter (Kluwer, Dortrecht, 1994).
[10] Z. Noszticzius, Q. Ouyang, W. D. McCormick, and H. L. Swinney, J. Phys. Chem. **96**, 6302 (1992).
[11] P. De Kepper, J. Boissonade, and I. R. Epstein, J. Phys. Chem. **94**, 6525 (1990).
[12] *CRC Handbook of Chemistry and Physics*, 50th ed. (Chemical Rubber, Cleveland, 1970), p. F-62.
[13] P. Manneville, *Dissipative Structures and Weak Turbulence* (Academic, New York, 1990), Chap. 8.
[14] Q. Ouyang, G. H. Gunaratne, and H. L. Swinney, Chaos **3**, 707 (1993); G. H. Gunaratne, Q. Ouyang, and H. L. Swinney, Phys. Rev. E **50**, 2802 (1994).
[15] I. Lengyel and I. R. Epstein, Science **251**, 650 (1991).